Strain engineering of epitaxially transferred, ultrathin layers of III-V semiconductor on insulator

Hui Fang,[1,2,3] Morten Madsen,[1,2,3] Carlo Carraro,[3,4] Kuniharu Takei,[1,2,3] Ha Sul Kim,[1,2,3] Elena Plis,[5] Szu-Ying Chen,[6] Sanjay Krishna,[5] Yu-Lun Chueh,[6] Roya Maboudian,[3,4] and Ali Javey[1,2,3,a)]

[1]*Electrical Engineering and Computer Sciences, University of California, Berkeley, California 94720, USA*
[2]*Materials Sciences Division, Lawrence Berkeley National Laboratory, Berkeley, California 94720, USA*
[3]*Berkeley Sensor and Actuator Center, University of California, Berkeley, California 94720, USA*
[4]*Chemical Engineering, University of California, Berkeley, California 94720, USA*
[5]*Department of Electrical and Computer Engineering and Center for High Technology Materials, University of New Mexico, Albuquerque, New Mexico 87106, USA*
[6]*Materials Science and Engineering, National Tsing Hua University, Hsinchu 30013, Taiwan*

(Received 23 November 2010; accepted 20 December 2010; published online 6 January 2011)

Strain state of ultrathin InAs-on-insulator layers obtained from an epitaxial transfer process is studied. The as-grown InAs epilayer (10–20 nm thick) on the GaSb/AlGaSb source wafer has the expected ~0.62% tensile strain. The strain is found to fully release during the epitaxial transfer of the InAs layer onto a Si/SiO_2 substrate. In order to engineer the strain of the transferred InAs layers, a ZrO_x cap was used during the transfer process to effectively preserve the strain. The work presents an important advance toward the control of materials properties of III-V on insulator layers. © *2011 American Institute of Physics*. [doi:10.1063/1.3537963]

III-V compound semiconductors have been extensively explored in the recent years for energy-efficient and high-speed electronics due to their high electron mobility and saturation drift velocity.[1–3] In this aspect, ultrathin, fully depleted layers are desired to reduce device leakage (i.e., off-state) currents, especially since many high mobility III-V semiconductors exhibit small bandgaps. Recently, the epitaxial transfer[3–5] of ultrathin (thickness, h_{InAs}=8–48 nm) InAs layers on Si/SiO_2 substrates was demonstrated by our group with the subsequently fabricated field-effect transistors exhibiting excellent electrical properties.[3] This compound semiconductor on insulator (termed XOI) technology presents a viable route toward the heterogeneous integration of III-V semiconductors on Si substrates without the use of complex heteroepitaxial growth processes. Of particular importance is to explore the strain state of the ultrathin XOI layers, and more crucially, to control it since strain plays a critical role in the electronic properties of materials.[6] Specifically, strain directly tailors the band offsets and carrier mobility by lifting the degeneracy in the bands which have been thoroughly investigated for heteroepitaxially grown multilayers.[6–8] In this paper, we investigate the strain state of ultrathin InAs XOI layers and demonstrate strain engineering by the use of a ZrO_x capping layer during the epitaxial transfer process.

The fabrication process for the InAs XOI substrates is shown schematically in Fig. 1(a) as previously reported in Ref. 3. Briefly, InAs thin films (h_{InAs}=10–20 nm) were grown epitaxially on a 60 nm thick $Al_xGa_{1-x}Sb$ (x=0.2–1) sacrificial layer on GaSb (001) substrates. The ultrathin InAs layers were lithographically patterned (width of 350 nm–5 μm) and wet etched using a mixture of citric acid [1 g/ml in de-ionized (DI) H_2O] and hydrogen peroxide (30%) at 1:20 volume ratio. Subsequently, the AlGaSb sacrificial layer was selectively etched in ammonium hydroxide (1.5%, in DI H_2O) solution. The partially released InAs micro- or nanoribbons [Fig. 1(b)] were transferred onto Si/SiO_2 receiver substrates using an elastomeric polydimethylsiloxane substrate (~2 mm thick). In order to engineer the strain of

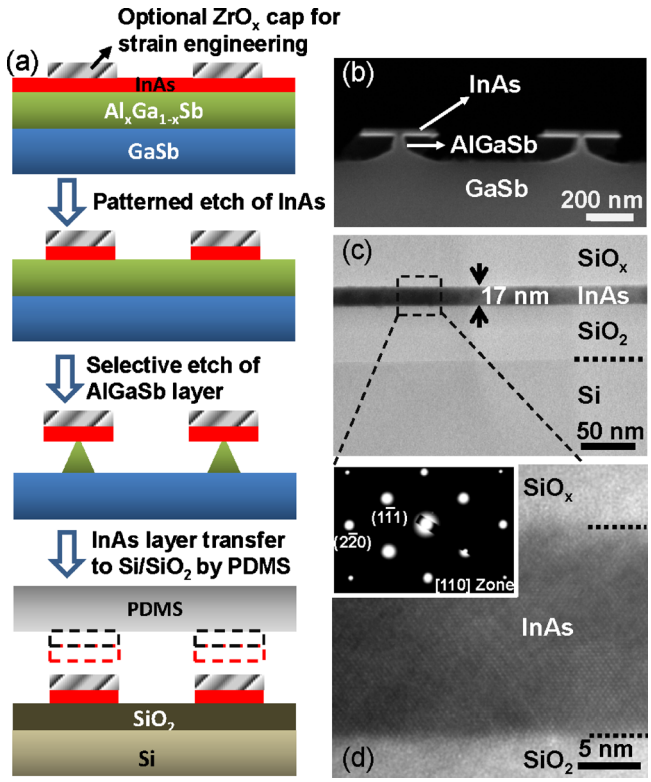

FIG. 1. (Color online) (a) The process schematics for epitaxial layer transfer of InAs thin films to Si/SiO_2 substrates. (b) Cross-sectional SEM image of InAs ribbons on the source wafer after the partial etch of the AlGaSb sacrificial layer and prior to the transfer. (c) and (d) Cross-sectional TEM images of an InAs XOI substrate (without ZrO_x cap).

a)Electronic mail: ajavey@berkeley.edu.

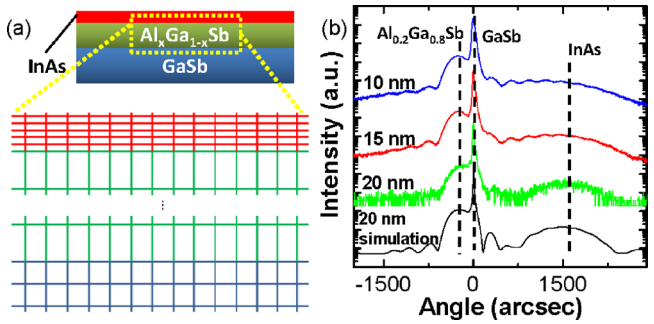

FIG. 2. (Color online) (a) The structure of GaSb/AlGaSb/InAs source wafer with an assumed strain state for each layer. (b) HRXRD spectra (referenced to GaSb substrate peak) of GaSb/$Al_{0.2}Ga_{0.8}Sb$/InAs source wafer with different InAs thicknesses.

transferred InAs layers, a ZrO_x (or SiO_x) capping layer was deposited by electron-beam evaporation on top of the source wafer prior to the epitaxial transfer process [Fig. 1(a)]. ZrO_x was chosen as the cap material because (1) ZrO_x is known to have a good interface with InAs (Ref. 3) which is beneficial for the eventual device fabrication and (2) ZrO_x has a large Young's modulus (130–250 GPa).[9] The cap prevents the relaxation of strain in InAs during the XOI fabrication process as shown later in detail in this paper. Figures 1(c) and 1(d) show the transmission electron microscopy (TEM) images of an InAs XOI substrate, clearly depicting the single-crystalline structure of the InAs layer on an amorphous SiO_2 layer. No clear voids are evident at the InAs interfaces, although it should be warned that TEM analyzes only a small cross-sectional area.

The structure of the source wafer is shown schematically in Fig. 2(a), with both InAs and AlGaSb layers coherently strained to the GaSb (001) substrate as confirmed by high resolution x-ray diffraction (HRXRD). Specifically, we used Ω-2θ coupled scan, where Ω is the incident angle between the x-ray source and the sample and 2θ is the diffraction angle between the incident beam and diffraction beam, to resolve the (004) peaks from InAs, AlGaSb, and GaSb and extract the out-of-plane lattice parameters, $a_\perp$. Figure 2(b) shows the diffraction spectra taken from GaSb/$Al_{0.2}Ga_{0.8}Sb$/InAs source wafers with h_{InAs}=10, 15, and 20 nm, referenced to the peak of GaSb substrate, which has a (004) Bragg angle at 30.3±0.1°. Using Bragg's law $2d \sin\theta = n\lambda$, where d is the distance between the (004) crystal plane ($d=a_\perp/4$), $n=1$, and λ is the x-ray wavelength (Cu's Kα), one obtains $a_\perp \sim 6.02$ and 6.11 Å for InAs and $Al_{0.2}Ga_{0.8}Sb$, respectively (note that $a_{\perp,GaSb} \sim 6.10$ Å, which is the bulk GaSb lattice parameter). From the equation $a_\parallel = C_{11}(a_0 - a_\perp)/2C_{12} + a_0$, where C_{11} and C_{12} are the elastic compliance constants[10] and a_0 is the bulk lattice parameter ($a_{0,AlxGa1-xSb} = (6.0959 + 0.0396x)$ Å, $a_{0,InAs} = 6.0584$ Å),[11] the in-plane lattice parameter $a_\parallel$ for both InAs and $Al_{0.2}Ga_{0.8}Sb$ layers is found to be ~6.10 Å, which is the same as that of GaSb (001). The experimental spectra also precisely match the simulation data [Fig. 2(b)], which assume that both $Al_{0.2}Ga_{0.8}Sb$ and InAs layers are biaxially strained such that their $a_\parallel$'s are the same as that of the GaSb substrate. The result is consistent with the fact that the thicknesses of the AlGaSb sacrificial layer and the InAs layer are within their theoretical critical thicknesses for heteroepitaxy of $h_c \sim 10.2$ μm and 240 nm for $Al_{0.2}Ga_{0.8}Sb$ and InAs, respectively, which can be calculated from the empirical equation $h_c = [A/(\Delta a/a_0)]^n$, where $A=16$ and $n=2.4$ for III-V's,[12] and Δa is the difference between $a_{0,AlxGa1-xSb}$ or $a_{0,InAs}$ and $a_{0,GaSb}$. The results are found to be generally true, regardless of the thickness of InAs and the Al content of the sacrificial layer used in this work. The amount of tensile strain inside the ultrathin InAs layer on the source wafers can be calculated by $\varepsilon_0 = (a_{0,GaSb} - a_{0,InAs})/a_{0,InAs} \sim 0.62\%$.

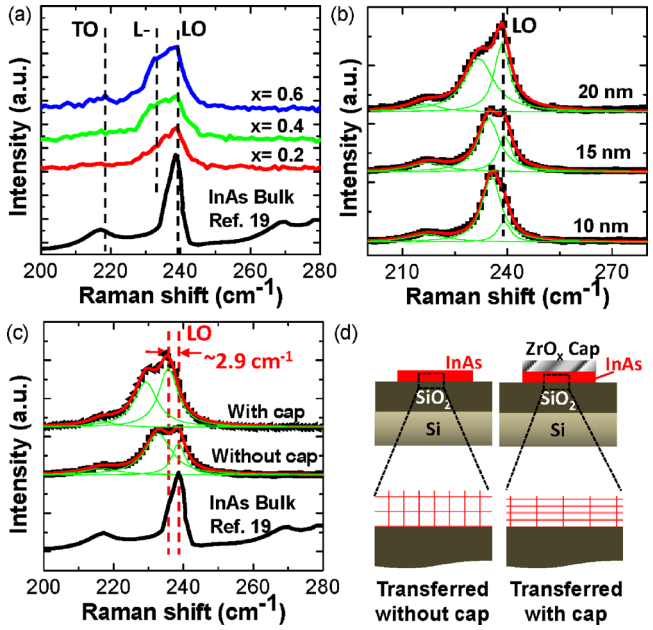

FIG. 3. (Color online) (a) Raman spectra of XOI samples (h_{InAs}=20 nm) obtained from GaSb/$Al_xGa_{1-x}Sb$/InAs source wafers with x=0.2, 0.4, and 0.6. (b) Raman spectra of XOI samples with different InAs thicknesses. (c) Raman spectra of relaxed and strained InAs XOI samples when transferred with and without the use of a ZrO_x capping layer. Lorentzian fitting was performed to extract the exact peak locations. (d) Schematic illustrations showing the lattices of relaxed and strained InAs XOI (not drawn to scale).

To visualize the strain state of the InAs layer in the XOI system (i.e., after transfer on Si/SiO_2 substrate), micro-Raman spectroscopy was employed. Note that Raman spectroscopy could not be used for the analysis of the source wafer since InAs, AlGaSb, and GaSb have overlapping peaks. Figure 3(a) shows the Raman spectra of InAs XOI (h_{InAs}=20 nm) obtained from source wafers with different composition of $Al_xGa_{1-x}Sb$ sacrificial layers (x=0.2, 0.4, and 0.6) along with the [001] bulk InAs data from literature.[13] Here, no capping layer was used during the epitaxial transfer process. The spectra distinctly depict the first order transverse optic mode (~217 cm^{-1}), longitudinal optic (LO) mode (~239 cm^{-1}), and the low frequency branch of coupled LO-phonon-plasmon mode (L-) (~230–235 cm^{-1}) phonon peaks[13–15] of InAs XOI. Clearly, InAs XOI layers obtained from sacrificial layers with different compositions exhibit near identical Raman spectra, with the LO peak position at ~239 cm^{-1} which is the same as that for the InAs bulk substrate [Fig. 3(a)]. Furthermore, the position of the LO peak is identical for InAs with thicknesses h_{InAs} =10–20 nm [Fig. 3(b)]. The results suggest that in the absence of a ZrO_x capping layer, the strain is fully released during the epitaxial transfer process. We hypothesize that the strain is released upon the partial etch of the AlGaSb layer, which results in nearly free-standing InAs layers [Fig. 1(b)]. The L-peak, which is due to the surface plasmon-LO phonon

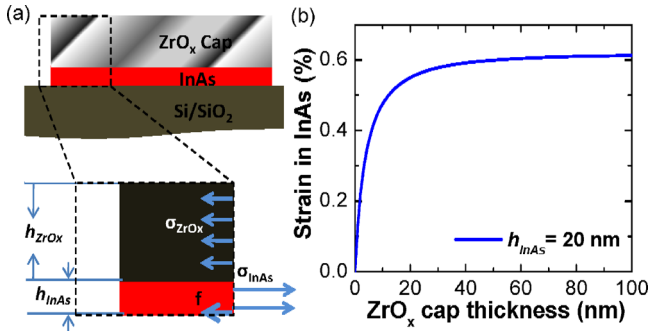

FIG. 4. (Color online) (a) Schematic of the stress distribution across a cross-section of ZrO_x cap and InAs layer. σ_{ZrOx} and σ_{InAs} are the normal stresses in ZrO_x and InAs, respectively, f is the force applied to the InAs layer from the substrate to neutralize the total force. (b) The dependence of the strain (ε) in the InAs XOI layer (h_{InAs}=20 nm) on the ZrO_x cap thickness (h_{ZrOx}).

coupling,[15] however, exhibits a h_{InAs} dependence [Fig. 3(b)]. One possible reason for the increasing L-/LO intensity ratio with reducing InAs thickness is due to the enhancement of the surface area to volume ratio. For all measurements, the intensity of the Raman laser power was decreased until the peak positions did not show any dependence on the laser intensity. This ensured a more accurate estimation of the phonon peak locations, without laser-induced heating.

A redshift of 2.9 ± 1.1 cm^{-1} in the LO peak position is clearly evident for InAs XOI layers transferred with a 70 nm ZrO_x cap as compared to those without a cap [Fig. 3(c)]. The amount of tensile strain inside the InAs XOI layer transferred with a cap was extracted from $\Delta\omega/\omega = (K_{11}/2)\varepsilon_{zz} + (K_{12}/2)(\varepsilon_{xx}+\varepsilon_{yy})$, where ω is the LO peak location (238.6 cm^{-1}), $\Delta\omega$ is the LO peak shift, K_{11} (-1.753×10^{11} dyn/cm^2), and K_{12} (-2.323×10^{11} dyn/cm^2) are the anharmonic spring constants for InAs LO phonon, and $\varepsilon_{xx} = \varepsilon_{yy}$, $\varepsilon_{zz} = -2C_{12}/C_{11}\varepsilon_{xx}$ are components of strain tensor inside InAs, with C_{11} (8.329×10^{11} dyn/cm^2) and C_{12} (4.526×10^{11} dyn/cm^2) as the elastic compliance constants of InAs.[10,16] From this analysis, we obtain an in-plane strain $\varepsilon_{xx} = \varepsilon_{yy} = 0.8 \pm 0.3\%$, which is within the expected range of the $\sim$0.62% initial strain of the as-grown InAs layer. We note that besides preserving the initial strain of the transferred InAs layer, the ZrO_x cap may also induce additional strain depending on its initial stress level upon evaporation.

To relate the amount of strain remaining in the InAs XOI layer to the ZrO_x cap thickness, analytical modeling was performed as shown in Fig. 4. For simplicity, it was assumed that the InAs and ZrO_x layers deform equally after release from the sacrificial layer and that the relationship between strain and stress is linear, given by Young's modulus E. Figure 4(a) schematically illustrates the stress distribution across a cross-section of the ZrO_x cap and InAs layer. The stress in each layer can be found by setting a common absolute deformation value, and the relationship between these two stresses can be set by zeroing the net moment caused by them. The remaining strain inside InAs is then determined by the following equation: $\varepsilon = mn(n+2)\varepsilon_0/[1+mn(n+2)]$, where $m = E_{ZrOx}/E_{InAs} \sim 2.63$ is the ratio of Young's moduli of ZrO_x and InAs, $n = h_{ZrOx}/h_{InAs}$ is the ratio of the thicknesses of ZrO_x and InAs, $\varepsilon_0 = 0.62\%$ is the as-grown InAs strain. The dependence of the strain (ε) in a 20 nm InAs layer on the cap thickness (h_{ZrOx}) is plotted in Fig. 4(b). The modeling indicates that the initial InAs strain is nearly fully maintained (by up to $\sim$98%) by a 70 nm ZrO_x cap, which is consistent with the experimental observations.

In conclusion, the strain state of InAs layers within the XOI platform was studied. The results highlight that the strain of the X layer in XOI can be tuned by choosing different cap layers (with different Young's moduli), cap thicknesses, and the initial stress inside the cap to obtain the optimal strain level for the desired device application. The presented approach adds yet another degree of versatility to the use of epitaxial layer transfer technique of ultrathin semiconductors for device applications.

This work was financially supported by MARCO/MSD Focus Center, NSF Energy Efficient Electronics Science Center, NSF (Grant No. DMR-0804646), AFOSR (Grant No. FA9550-09-1-0202, and Nation Science Council, Taiwan NSC (Grant No. 99-2628-E-007-006). The materials characterization of this work was funded by a LDRD from LBNL. A.J. acknowledges a Sloan research fellowship, and support from the World Class University program at Sunchon National University. M.M. acknowledges a postdoctoral fellowship from the Danish Research Council for Technology and Production Sciences.

[1] R. Chau, B. Doyle, S. Datta, J. Kavalieros, and K. Zhang, Nature Mater. **6**, 810 (2007).
[2] D.-H. Kim and J. A. del Alamo, IEEE Trans. Electron Devices **57**, 1504 (2010).
[3] H. Ko, K. Takei, R. Kapakia, S. Chuang, H. Fang, P. W. Leu, K. Ganapathi, E. Plis, H. S. Kim, S.-Y. Chen, M. Madsen, A. C. Ford, Y.-L. Chueh, S. Krishna, S. Salahuddin, and A. Javey, Nature (London) **468**, 286 (2010).
[4] E. Yablonovitch, D. M. Hwang, T. J. Gmitter, L. T. Florez, and J. P. Harbison, Appl. Phys. Lett. **56**, 2419 (1990).
[5] D.-H. Kim, Y.-S. Kim, J. Wu, Z. Liu, J. Song, H.-S. Kim, Y. Y. Huang, K.-C. Hwang, and J. A. Rogers, Adv. Mater. **21**, 3703 (2009).
[6] M. Chu, Y. Sun, U. Aghoram, and S. E. Thompson, Annu. Rev. Mater. Res. **39**, 203 (2009).
[7] M. M. Roberts, L. J. Klein, D. E. Savage, K. A. Slinker, M. Friesen, G. Celler, M. A. Eriksson, and M. G. Lagally, Nature Mater. **5**, 388 (2006).
[8] S. Suthram, Y. Sun, P. Majhi, I. Ok, H. Kim, H. R. Harris, N. Goel, S. Parthasarathy, A. Koehler, T. Acosta, T. Nishida, H.-H. Tseng, W. Tsai, J. Lee, R. Jammy, and S. E. Thompson, Proceedings of the IEEE Symposium on VLSI Technology, 2002, p. 182.
[9] J. F. Shackelford and W. Alexander, *Materials Science and Engineering Handbook*, 3rd ed. (CRC, Boca Raton, 2001), p. 511.
[10] T. Mozume, Mater. Res. Soc. Symp. Proc. **324**, 285 (1994).
[11] P. V. Neklyudov, S. V. Ivanov, B. Y. Mel'tser, and P. S. Kop'ev, Semiconductors **31**, 1067 (1997).
[12] S. Adachi, *Properties of Semiconductor Alloys: Group IV, III-V, and II-VI Semiconductors* (Wiley, New York, 2009), p. 39.
[13] R. Carles, N. Saint-Cricq, J. B. Renucci, M. A. Renucci, and A. Zwick, Phys. Rev. B **22**, 4804 (1980).
[14] N. Begum, M. Piccin, F. Jabeen, G. Bais, S. Rubini, F. Martelli, and A. S. Bhatti, J. Appl. Phys. **104**, 104311 (2008).
[15] S. Buchner and E. Burstein, Phys. Rev. Lett. **33**, 908 (1974).
[16] J. Groenen, A. Mlayah, R. Carles, A. Ponchet, A. Le Corre, and S. Salaun, Appl. Phys. Lett. **69**, 943 (1996).